JOURNAL OF MATERIALS SCIENCE 26 (1991) 1861–1866

Laser-induced deposition of thin chromium oxide films

E. JACOBSOHN*, J. ZAHAVI‡, A. ROSEN*, S. NADIV*
*Department of Materials Engineering, and ‡Israel Institute of Metals, Technion, I.I.T. Haifa, Israel

Molybdenum, 1045 carbon steel and silicon specimens have been coated with thin layers of Cr_2O_3 by means of ArF excimer pulse laser decomposition of $Cr(CO)_6$ gas. The results of the study revealed that the properties of the films, such as composition, thickness, morphology and microstructure depend on both the parameters of the laser radiation and the physical properties of the substrates.

1. Introduction

Laser-induced deposition out of a gaseous phase on various substrates has been intensively studied during recent years [1–3]. The main advantage of this method, compared to others, is the ability of the laser beam to act as a localized controllable heat and/or light source. Another advantage of the method is the ability to control the morphology, the dimensions and the thickness of the deposited layer, through the control of the energy which goes to the deposition reaction. These two factors allow direct writing of lines and various shapes of controlled depth and morphology, without the need to use elaborate masking procedures. Short-time pulse laser radiation has another advantage: since the area of contact between the laser beam and the substrate is small and the time interval is short, heat can only penetrate to very shallow depths, i.e., the damage caused by heating is minimal [4].

These properties are important mainly for applications in micro-electronics and naturally, most of the research is concentrated on the deposition of metals on semiconductors [1–3]. However, this technique can also be used for the coating of metallic substrates. In this investigation two different metals were used as substrates: plain carbon steel (SAE 1045) and molybdenum. For the sake of reference, silicon was also coated. The coating substance was chromium oxide. Part of this investigation, which deals with molybdenum has already been published [5] and reported here, is the complete study.

2. Experimental procedure

Fig. 1 shows the experimental set-up. It consists of the laser device, the cell and the optical system. The laser used in this investigation was an ArF excimer laser with wave length of 193 nm and pulse duration of 24 ns. The specimen was placed into the cell, which also contained chromium–carbonyl [$Cr(CO)_6$] crystals placed on a hot plate. First a vacuum of 0.1333 Pa was created and then the cell was heated to 50 °C which is equivalent to the chromium–carbonyl vapour pressure of 2.13×10^2 Pa. The next step was to fill up the cell with high purity argon gas until atmospheric pressure was reached. Laser irradiation was done normal to the specimens surface. The variables of the experiments were the power density (10–120 MW cm^{-2}) and the number of pulses (100–6000). The repetition rate has been kept constant, 4 Hz.

The substrate materials were: SAE 1045 carbon steel in normalized condition, molybdenum and silicon single crystal, (1 1 1) orientation. The metal–substrates were metallographically polished.

3. Results

3.1. Effect of power density and number of pulses on the chromium content of the deposited layer

The qualitative assessment of the amount of chromium in the deposited layer was performed by scanning electron microscopy (SEM) equipped by energy dispersive system (EDS). The maximum thickness of the deposited layer was 5000 nm, while the penetration depth of EDS is approximately one micrometre. This means that the depth of the EDS excited volume is an order of magnitude larger than the thickness of the film and therefore the measurements give the total amount of chromium in a certain volume.

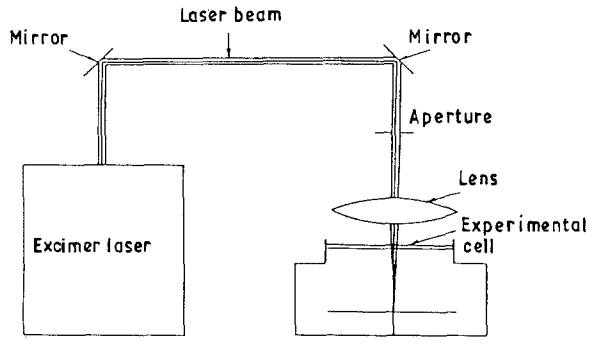

Figure 1 Schematic illustration of the experimental set-up.

0022–2461/91 $03.00 + .12

Fig. 2 shows the atomic percentage of chromium deposited on the various substrates versus the number of pulses for the molybdenum, steel and silicon, respectively. The power density is indicated in the diagrams. Within the range of experiments the relationship between the Cr concentration and the number of pulses is linear and except for the steel sample, all the results extrapolate to the origin.

The amount of chromium in the deposited layer versus power density for constant number of pulses (2000) is shown in Fig. 3 for the three substrates. These diagrams actually exhibit the variation of the deposition rate with the power density. This relationship is not linear, but a declining function. The power density at which the deposition rate starts to decline is dependent on the type of substrate. In both, Figs 2 and 3, the concentration of Cr in the silicon substrate is much lower than in the metallic substrates. This is not a real effect, but it is a result of the deep penetration of EDS into silicon, compared to metals.

3.2. The dependence of layer thickness on power density and number of pulses

The thickness of the layers has been measured by means of Auger spectroscopy (AES). Fig. 4a–c exhibit

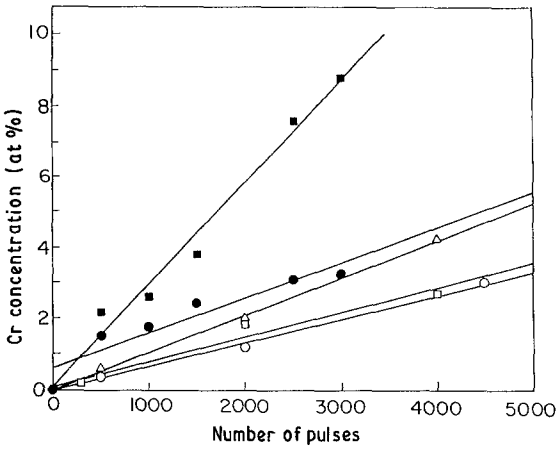

Figure 2 The variation of the chromium concentration in the deposited layer with the number of pulses, for the substrates of (a) molybdenum (■) 54, (□) 18.7 MW cm^{-2}, (b) steel (●) 22 MW cm^{-2} and (c) silicon (○) 24, (△) 57 MW cm^{-2}.

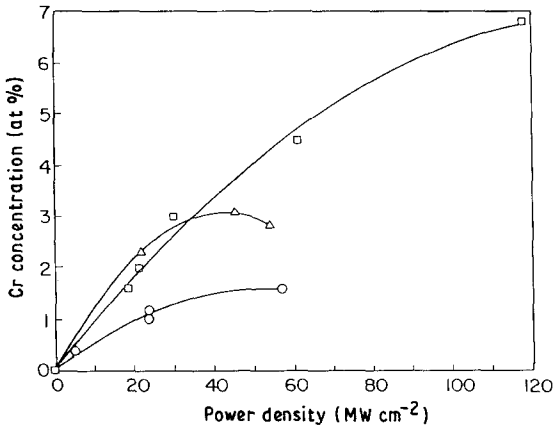

Figure 3 The variation of chromium concentration in the deposited layer with the power density at 2000 pulses for the substrates of (□) molybdenum, (△) steel and (○) silicon.

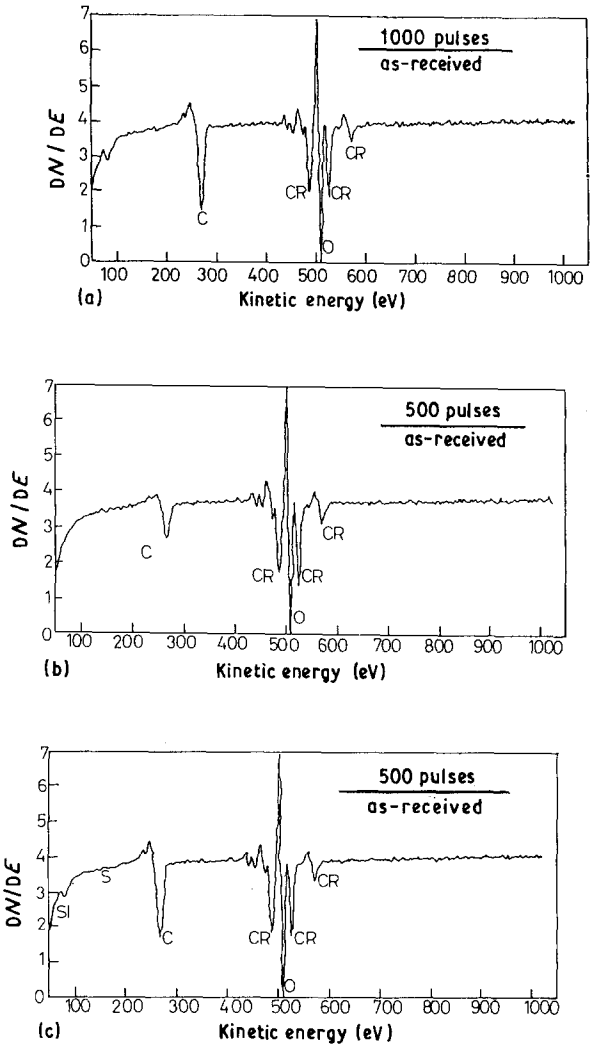

Figure 4 AES spectrum, before sputtering, for the substrates of (a) molybdenum, (b) steel and (c) silicon.

the AES spectrum for the three substrates before sputtering. The number of pulses and the power density of deposition are indicated in the diagrams. For the metal samples the surface layer of the coating contained no Mo or Fe, however the surface layer of the coating on the silicon substrate contained Si.

Figs 5 and 6 exhibit the AES compositional depth profiles for the molybdenum substrate, i.e., the variation of the films composition with sputtering time. While Fig. 5 demonstrates the effect of number of pulses, Fig. 6 shows the effect of power density. Fig. 7 presents the same data for the steel substrate (only for the power density of 22 MW cm^{-2}). Figs 8 and 9 stand for the silicon substrate, where Fig. 8 represents the effect of number of pulses and Fig. 9 exhibits the influence of the power density. As mentioned before, the chromium oxide coating on the silicon substrate contains Si. This can be clearly seen in Figs 8 and 9. These figures also show that the concentration of Si in the coatings increases with the power density of deposition. Another feature typical of the silicon substrate is that at some distance from the surface the concentration of oxygen becomes lower than that of the chromium. For the metallic substrates the oxygen concentration is higher than the chromium concentration.

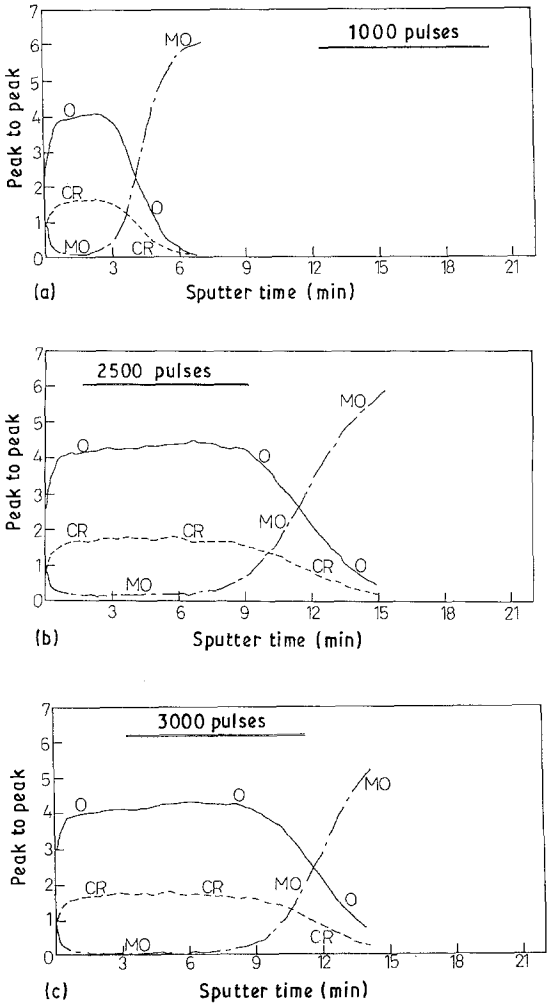

Figure 5 The effect of number of pulses on AES compositional depth profiles for molybdenum substrate.

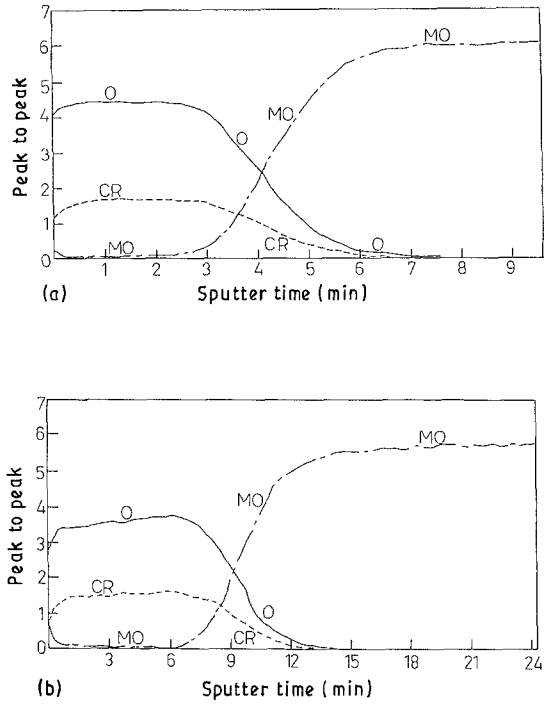

Figure 6 The effect of power density on AES compositional depth profiles for molybdenum substrate; (a) 20.8 and (b) 36.8 MW cm^{-2}.

3.3. Morphology and microstructure of the deposited surface

Fig. 10a and b show SEM micrographs of a steel substrate after deposition with a power density of 13 MW cm^{-2} after 300 and 400 pulses, respectively. The scratches seen on the micrographs are due to rough polishing in order to enlarge surface absorption. Fig. 11a and b depict molybdenum substrates which were deposited at a constant pulse number of 2000, with power densities of 61 and 119 MW cm^{-2}. These micrographs are representing all the other substrates under similar conditions.

For relatively low power densities, for example 20 MW cm^{-2} for steel or 40 MW cm^{-2} for molybdenum, the film starts to build up from tiny spots, such as shown in Fig. 10. The size and density of the spots increases with the number of pulses. When the power

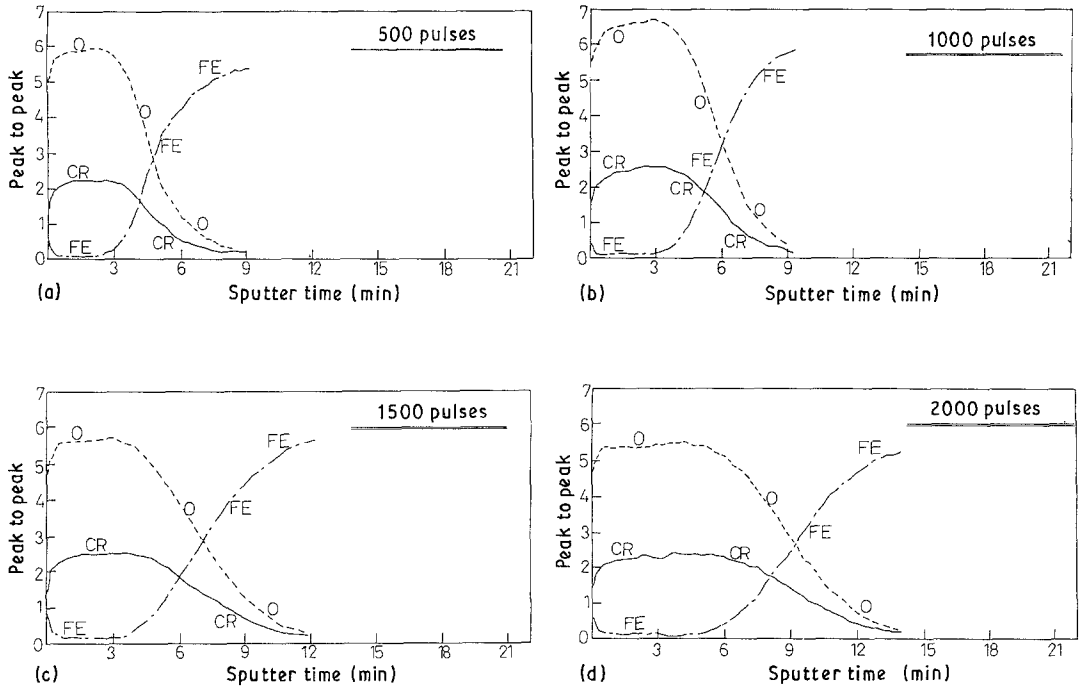

Figure 7 The effect of number of pulses on AES compositional depth profiles for steel substrate (power density 22 MW cm^{-2}).

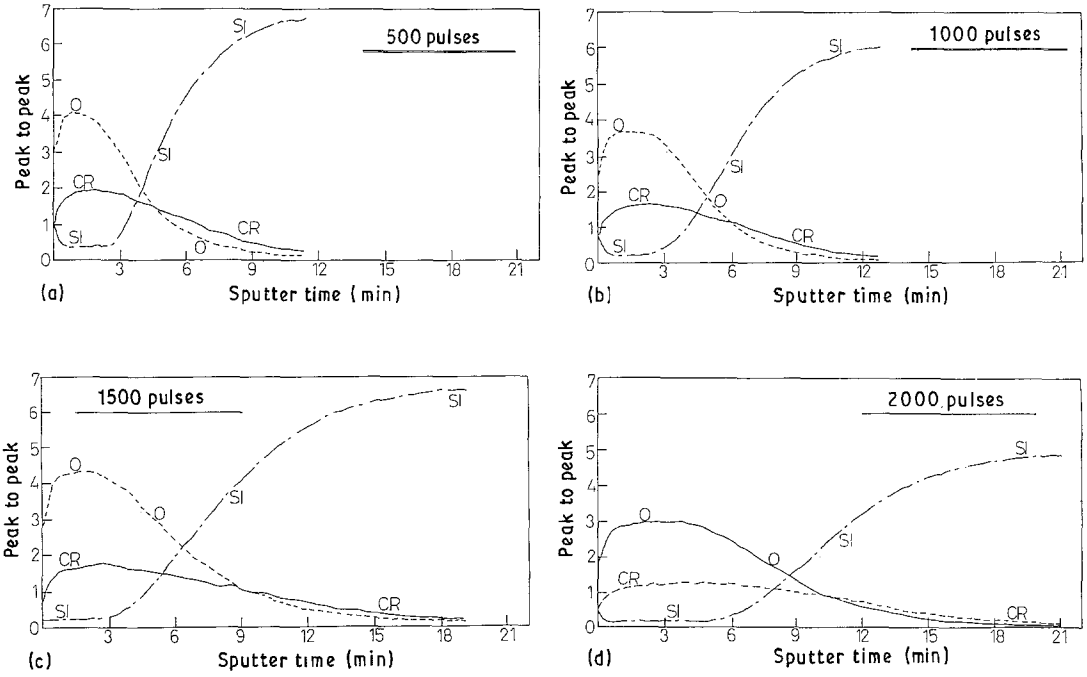

Figure 8 The effect of number of pulses on AES compositional depth profiles for silicon substrate.

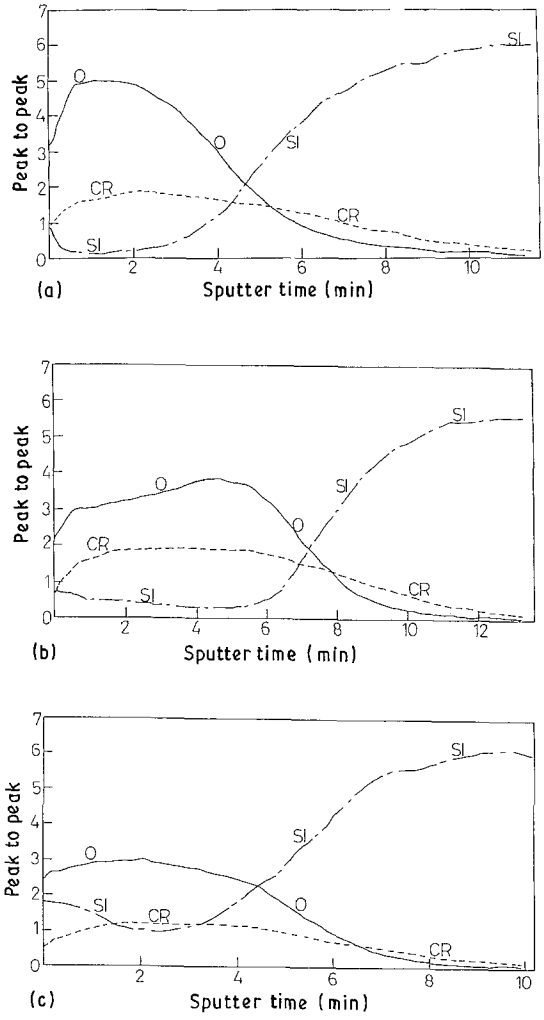

Figure 9 The effect of power density on AES compositional depth profiles for silicon substrate; (a) 17.9, (b) 31 and (c) 60 MW cm^{-2}.

density increases, a continuous layer with a grain structure is obtained, as seen in Fig. 11a. For even higher power densities both the layer and the substrate were melted (Fig. 11b). The cracks in the picture

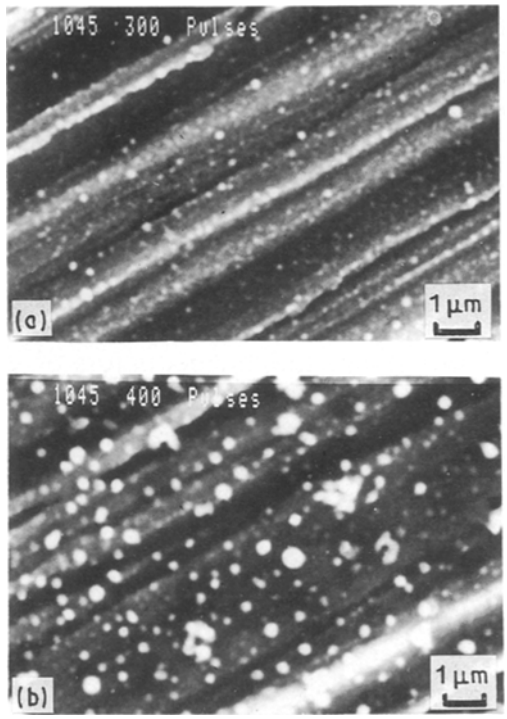

Figure 10 SEM photomicrographs of steel substrate after deposition with power density of 13 MW cm^{-2}, (a) 300 and (b) 400 pulses.

are probably the result of very high heating and cooling rates.

4. Discussion

The purpose of this investigation was to understand the mechanism and to study the feasibility of coating metallic and non-metallic surfaces with chromium oxide from a gaseous substance by utilizing laser energy.

For each substrate, the amount of chromium in the deposited layer varies linearly with the number of

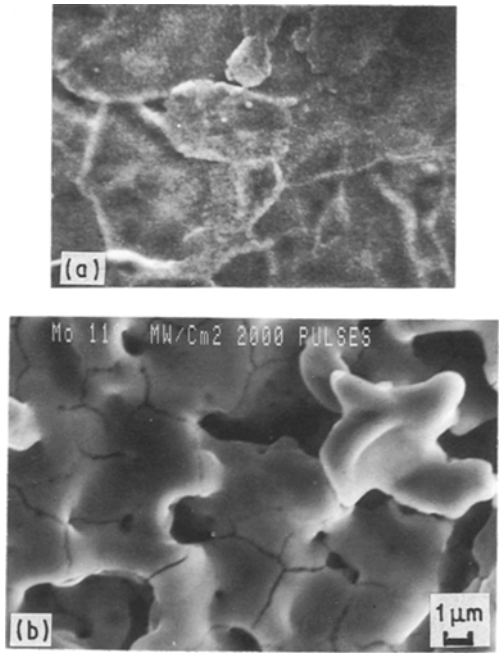

Figure 11 SEM photomicrographs of molybdenum substrate after 2000 pulses, with power densities of (a) 61 and (b) 119 MW cm^{-2}.

pulses. This result indicates that each pulse decomposes an equal amount of chromium from the chromium–carbonyl atmosphere and deposit it on the substrate. This result is consistent with the model proposed by Esrom and Wahl [6] for pyrolytic mechanism and also with the model of Chen [3] for the photolytic mechanism. The substance of the substrate does not effect the mechanism of deposition.

The variation of the chromium concentration in the deposited layer with the power density is not a linear function, but a declining one. There are several causes which can account for the saturation of the deposition rate with high power density: (i) evaporation of the coating due to high power radiation [7], (ii) limitation in the mass transport of the reacting gas and (iii) deposition of the chromium on the cell window, which lowers the effective power density [8].

The AES compositional depth profiles (Figs 5 to 9) revealed high concentration of silicon, as well as oxygen in the coatings of the silicon substrates but no iron or molybdenum in the coatings of the metallic substrates. It is suggested that silicon from the substrate diffused into the chromium oxide layer through grain boundaries during the deposition process, and oxidized into SiO_2. The rate of diffusion of the silicon increased with increasing power density. Lien *et al.* [9] have reported that oxygen inhibits the formation of chromium silicides in a Si–Cr system even after 2 h at 450 °C. The mobile atoms in this system were the silicon atoms rather than the chromium atoms. Experiments performed with ruby pulse lasers have shown that the melt life of silicon is long enough to allow diffusion to occur [10]. These experiments may explain the diffusion of silicon into the deposited layer and also the fact that no sign of silicide formation was observed.

The composition of the coatings, as evidenced by AES and low angle X-ray diffraction (LAXD) was Cr_2O_3 on all the substrates. Several investigators obtained similar results [11], even when experiments were conducted in high vacuum. It can be assumed therefore that the formation of a chromium oxide layer is a result of the decomposition of chromium–carbonyl.

It is possible to calculate the approximate maximum temperature due to laser irradiation [2]

$$T = P(1 - R_s)/(2\pi w_o k) \quad (1)$$

where P is the intensity of the incident beam, R_s is the surface reflectivity, k is the thermal conductivity of the substrate and w_0 is the laser spot size. Equation 1, which has been developed for continuous laser radiation, can also be used for pulse laser, with the following modification [2]

$$T_p = 2/\pi\, T \tan^{-1}(2D_{th}t_p/w_o) \quad (2)$$

In this equation D_{th} is the thermal diffusivity of the substrate and t_p is the pulse duration.

Equation 2 shows that the thermal properties of the substrate play an important role, since the temperature of the surface is not only affected by the power density of the laser beam but also by the thermal properties of the substrate. Table I shows the dependence of the film thickness on the thermal properties of the substrate. The conditions of irradiation were 2000 pulses at a power density of 20 MW cm^{-2}.

Table I shows that the thermal diffusivity of Mo and Si are eventually the same while the reflectivity of the two metals are identical. Thermal diffusivity determines the ability of a given material to absorb and to transfer thermal energy. Carbon steel has the lowest thermal diffusivity and therefore its surface temperature will be the highest among the three. Higher surface temperature results in a higher pyrolytic reaction rate and thicker films. Silicon, like molybdenum, also has a high thermal diffusivity, however its reflectivity is low. For this reason, the substrate of silicon absorbs more energy and therefore allows thicker coating than molybdenum.

TABLE I The dependence of film thickness on the thermal properties of a substrate

Substrate	Thermal diffusivity ($cm^2\ s^{-1}$) [12]	Reflectivity [5]	Film thickness[a] (nm)
1045 steel	0.21	0.9	3600
molybdenum	0.51	0.9	2000
silicon	0.53	0.6	3400

[a] The thickness of the chromium oxide layer on the different substrates was determined arbitrarily, as the distance where the concentration of chromium is one-half of that on the surface.

All the experiments were performed with the laser beam normal to the substrate and therefore its surface temperature increases during the process. Elevated temperature slows down the nucleation rate but on the other hand enhances the growth rate of the film. The rate of nucleation is therefore the rate controlling process and the films grow as single layers, such as shown in Fig. 11a. In extreme cases, for example very high power densities, the surface melts, like that shown in Fig. 11b. When the power density is low, the heating of the surface is minimal, and the film growth by accumulation of spots, e.g. Fig. 10a and b.

5. Conclusions

It has been demonstrated that chromium oxide layers of various thicknesses can be deposited on metallic or non-metallic surfaces by means of ArF eximer pulse laser. The deposition is obtained by the decomposition of chromium–carbonyl under controlled conditions of laser beam power density and the number of pulses. The investigation revealed the following facts:

1. The morphology of the coatings depends on the power density. At low densities the film is built by tiny, scattered spots, while at higher densities a continuous layer is obtained. At very high power densities both the substrate and the film melt.

2. Within the range of the experiments, the chromium concentration of the coatings increases linearly with the number of pulses.

3. The chromium concentration of the coatings is an asymptotic function of the power density. At a certain power density, depending on the physical properties of the substrate, saturation occurs and further growth is limited.

4. The film thicknesses under identical deposition conditions depend on the physical properties of the substrate, such as their reflectivity and thermal diffusivity.

Acknowledgements

The authors would like to take the opportunity to thank the following persons for their help with the various phases of the investigation: Mrs S. Tamir, Dr M. Fishman and Mrs M. Rotel of IIM, Mr A. Roth and Mr S. Altshulin of DME.

References

1. D. J. ERLICH and J. Y. TSAO, *J. Vac. Sci. Technol.* **B1** (1985) 969.
2. Y. RYTZ-FROIDEVAUX, R. P. SALATHE and H. H. GILGEN, *Appl. Phys.* **A37** (1985) 121.
3. C. J. CHEN, *J. Vac. Sci. Technol.* **A5** (1987) 3386.
4. C. W. WHITE and M. J. AZIZ, in "Surface Alloying by Ion, Electron and Laser Beams", edited by L. E. Rehn, S. T. Picraux and H. Wiedesich (ASM, Ohio, USA, 1986) p. 19.
5. E. JACOBSOHN, J. ZAHAVI, A. ROSEN and S. NADIV, in The 12th International Plansee Seminar, edited by H. Bildstein and H. M. Ortner (Metalwerk Plansee GmBH, Revtte, Austria, 1989) p. 109.
6. H. ESROM and G. WAHL, in Proceedings of the 6th European Conference on CVD, edited by R. Porat (Iscar Ltd, Israel, 1987) p. 367.
7. R. K. KRCHNAVEK, H. H. GILGEN, J. C. CHEN, P. B. SHAW, T. J. LUCATU and P. M. OSGOOD, Jr, *J. Vac. Sci. Technol.* **B5** (1987) 20.
8. I. P. HERMAN, R. A. HYDE, B. M. McWILLIAMS and L. L. WOOD, in MRS Symposium Proceedings (Elsevier Science, New York, 1983) p. 9.
9. C. D. LIEN, L. S. WIELUNSKI, M. A. NICOLET and K. M. STIKA, in MRS Symposium Proceedings, edited by R. Ludeke and K. Rose (North Holland, New York, 1983) p. 235.
10. G. J. GALVIN, M. O. THOMPSON, J. W. MAYER, P. S. PERCY, R. B. HAMMOND and N. PAULTER, *Phys. Rev.* **B27** (1983) 1079.
11. P. J. LOVE, R. T. LODA, P. R. LA ROE, A. K. GREEN and V. RHEN, in "Laser Controlled Chemical Processing of Surfaces", Vol. 29, edited by A. W. Johnson, D. J. Erlich and H. R. Schlossberg (Elsevier Science, New York, 1984) p. 101.
12. J. F. READY, in "Industrial Applications of Lasers" (Academic, New York, 1978) p. 341.

Received 2 January
and accepted 16 May 1990